

## Critical behavior of the thermal properties of $\text{KMnF}_3$

A. Salazar,\* M. Massot, and A. Oleaga

*Departamento de Física Aplicada I, Escuela Técnica Superior de Ingeniería, Universidad del País Vasco, Alameda Urquijo s/n, 48013 Bilbao, Spain*

A. Pawlak

*Institute of Physics, A. Mickiewicz University, 61-614 Poznan, Poland*

W. Schranz

*Faculty of Physics, University of Vienna, Strudlhofgasse 4, A-1090 Wien, Austria*

(Received 14 March 2007; published 27 June 2007)

An ac photopyroelectric calorimeter has been used to simultaneously measure the specific heat, thermal conductivity, and thermal diffusivity around the antiferromagnetic to paramagnetic phase transition in  $\text{KMnF}_3$ . It has been found that the critical exponent and the amplitude ratio of the thermal diffusivity are the same as those of the specific heat. Both values agree with the predictions of the three-dimensional Heisenberg model for isotropic magnets, although this transition is not only magnetic but also structural as well. The thermal conductivity shows a broad peak at the Néel temperature that could be related to a reduction of the phonon scattering by the spin fluctuation as the transition temperature is approached.

DOI: 10.1103/PhysRevB.75.224428

PACS number(s): 75.40.-s, 75.50.Ee, 64.60.Ht, 65.40.-b

### I. INTRODUCTION

The critical phenomena associated with static quantities, such as specific heat ( $c_p$ ), at magnetic phase transitions have been widely studied in the past. Most experimental results confirm the universality hypothesis which states that the critical behavior depends only on the dimensionality of the system ( $d$ ) and on the degree of freedom of the order parameter ( $n$ ). For instance, antiferromagnetic materials, provided that only short-range interactions are relevant, can be described by a Heisenberg model if  $d=3$  and  $n=3$  (isotropic), by an  $XY$  model if  $d=3$  and  $n=2$ , and by an Ising model if  $d=3$  and  $n=1$  (uniaxial anisotropic). On the contrary, in the case of dynamics quantities, such as the thermal conductivity ( $K$ ) and the thermal diffusivity ( $D$ ), few high-resolution data for solid samples are available in the literature.<sup>1-6</sup> This is due to the conflict between the need of producing thermal gradients for thermal transport measurements and the need of keeping them as small as possible so as not to destroy the critical information. In this way, the ac photopyroelectric calorimetry<sup>7,8</sup> is specially suited for the measurement of the thermal transport properties around phase transitions, since small temperature gradients in the sample produce a good signal-to-noise ratio, letting thermal properties be measured with high accuracy. Measurements on the uniaxial antiferromagnet  $\text{FeF}_2$  show that the critical exponents and amplitude ratios of thermal diffusivity ( $b$ ,  $U^+/U^-$ ) and specific heat ( $\alpha$ ,  $A^+/A^-$ ) satisfy the relations<sup>3</sup>  $b=-\alpha=-0.11$  and  $U^+/U^-=A^+/A^-=2.0$ , in agreement with the prediction of the so-called model  $C$ , for which the energy is conserved.<sup>9,10</sup> Superscripts  $+$  and  $-$  correspond to measurements above and below the transition temperature, respectively. However, the thermal conductivity shows a broad peak in the vicinity of the transition temperature but no clear anomaly was detected. Measurements on  $\text{RbMnF}_3$ , a well known isotropic antiferromagnet, gave<sup>5</sup>  $b=\alpha=-0.11$  and  $U^+/U^-=A^+/A^-=1.27$ , in agreement with recent calculations by Pawlak.<sup>10</sup> In thermal

conductivity, a small anomaly was found with a cusplike maximum and no divergence. As for both kinds of antiferromagnets (uniaxial and isotropic) the critical exponents for thermal diffusivity are the same ( $b=-0.11$ ), the important information about anisotropy lies in the amplitude ratio and in the magnitude of the regular term.

In this work, we use a photopyroelectric calorimeter to simultaneously measure  $c_p$ ,  $K$ , and  $D$  in  $\text{KMnF}_3$ . At room temperature, it has a perovskite cubic structure, but unlike  $\text{RbMnF}_3$ , it undergoes several structural phase transitions as the temperature decreases. In particular, at 88 K, a change from tetragonal to orthorhombic structure is superimposed to the antiferromagnetic to paramagnetic transition. Our aim is to study the critical behavior of the thermophysical parameters near the magnetic transition as well as the influence of the nearby structural transition on these parameters. Actually, previous  $c_p$  measurements gave critical exponent values that are rather far from those predicted in the three-dimensional (3D) Heisenberg model:  $\alpha=-0.16$  and  $\alpha=-0.19$ .<sup>11,12</sup> Moreover, as far as we know, no high-resolution measurements of  $D$  and  $K$  close to the magnetic transition have been performed. It is worth noting that the possibility of a simultaneous measurement of both static and dynamic quantities on the same sample under the same experimental conditions, such as thermal gradients, heating rate, etc., can greatly help when using the results of the measurements in scaling laws. Our results indicate that the critical behavior of  $c_p$  and  $D$  agrees with the 3D Heisenberg model and are not affected by the presence of the structural phase transition. Data on thermal conductivity showing a broad peak are also reported.

### II. SAMPLE CHARACTERISTICS

The density at room temperature is  $3.42 \text{ g/cm}^3$ . Pure  $\text{KMnF}_3$  has a perovskite structure and undergoes three structural phase transitions related to the rotation of the octahedra at the following temperatures: 186.5, 88, and 82 K.<sup>13</sup> At high

temperature,  $\text{KMnF}_3$  shows a cubic phase with space group ( $Pm\bar{3}m$ ). Below 186.5 K, it becomes tetragonal ( $I4/mcm$ ) with the tetragonal  $c$  axis developing around the axis of rotation of the octahedra ( $c/a > 1$ ), namely, one of the [001] cubic axes. At 88 K, it changes to an orthorhombic phase ( $Pnma$ ) in which the octahedra are still rotated around the previous tetragonal axis and slightly rotated around one of the tetragonal  $a$  axes. Finally, below 82 K, a tetragonal phase is developed in which the octahedra are rotated around all the [001] directions of the cubic phase.

Regarding its magnetic properties,  $\text{KMnF}_3$  becomes antiferromagnetic below the Néel temperature  $T_N = 88$  K and transforms further to a canted antiferromagnet at 82 K. According to various authors, an additional structural phase transition appearing at 91 K, very close to  $T_N$ , claimed either first order<sup>14</sup> or second order.<sup>15</sup> Kapusta *et al.*<sup>16</sup> confirm the presence of the transition at 91 K from tetragonal to monoclinic ( $P2_1/m$ ) instead of the transition at 83 K. However, no definitive consensus has been obtained yet.

Measurements of the uniaxial anisotropy (the ratio between the anisotropy field  $H_A$  and the exchange field  $H_E$ ) have shown different results:<sup>17,18</sup>  $H_A/H_E = 4.3 \times 10^{-3}$  and  $H_A/H_E = 5.9 \times 10^{-6}$ . According to the first value,  $\text{KMnF}_3$  is an anisotropic antiferromagnet like  $\text{MnF}_2$ , while according to the second one, it is an isotropic antiferromagnet, as was the case of other magnetic trifluorides such as  $\text{RbMnF}_3$  and  $\text{KNiF}_3$ .

Specific heat ( $c_p$ ) measurements around the magnetic phase transition show the typical lambda shape of a second order phase transition.<sup>11,12,19</sup> Only in the work of Khlyustov *et al.*<sup>19</sup> a singularity at 95 K, different from the magnetic one, is reported. Analysis of the critical behavior shows the following values for the critical exponent and the amplitude ratio:  $\alpha = -0.16$  and  $A^+/A^- = 1.73$  (Ref. 11) and  $\alpha = -0.19$  and  $A^+/A^- = 1.36$ .<sup>12</sup> Although these values point to a 3D Heisenberg universality ( $\alpha = -0.11$  and  $A^+/A^- = 1.58$ ), a crossover to 3D Ising universality is also found as the temperature approaches  $T_N$ .

Thermal conductivity ( $K$ ) measurements show a broad minimum near the Néel temperature which was firstly attributed to magnetic interactions.<sup>20,21</sup> However, Gustafson and Walker<sup>22</sup> have reported that the similar antiferromagnet  $\text{RbMnF}_3$ , which has no structural phase transitions, shows no anomalies in the thermal conductivity near  $T_N$ . Since  $\text{RbCaF}_3$ , which has similar structural transitions to those observed in  $\text{KMnF}_3$  but is nonmagnetic, shows a similar minimum in thermal conductivity, it was concluded that the reduction in the thermal conductivity is due to the enhanced phonon-phonon scattering due to the soft phonon modes and not to the spin-phonon coupling.<sup>23</sup> However, probably, the poor resolution in the thermal conductivity measurements is the reason why no magnetic anomaly has been measured previously. Accordingly, a high-resolution technique is needed to detect a variation in  $K$  in the vicinity of a magnetic transition in order to study its critical behavior.

### III. EXPERIMENTAL SETUP AND RESULTS

Simultaneous measurements of  $K$ ,  $D$ , and  $c_p$  have been performed by a high-resolution ac photopyroelectric calorim-

eter used in the standard back-detection configuration.<sup>7,8</sup> An acousto-optically modulated He-Ne laser beam of 5 mW illuminates the front surface of the sample under study. Its rear surface is in thermal contact with a 350  $\mu\text{m}$  thick  $\text{LiTaO}_3$  pyroelectric detector with Ni-Cr electrodes on both surfaces by using an extremely thin layer of a highly heat-conductive silicone grease (Dow Corning, 340 heat sink compound). The photopyroelectric signal is processed by a lock-in amplifier operating in the current mode. Both sample and detector are placed inside a nitrogen bath cryostat that allows measurements in the temperature range from 77 to 500 K at rates that vary from 100 mK/min for measurements on a wide temperature range to 10 mK/min for high-resolution runs close to the phase transitions.

For opaque and thermally thick samples (i.e., the thickness of the sample is higher than the thermal diffusion length  $\mu = \sqrt{D/\pi f}$ , where  $f$  is the modulation frequency of the light beam), the natural logarithm ( $\ln V$ ) and the phase ( $\Psi$ ) of the normalized photopyroelectric current (that is obtained dividing by the signal provided by the bare detector) have a linear dependence on  $\sqrt{f}$ , with the same slope. From their slope  $m$  and from the vertical separation between the two straight lines  $d$ , the thermal diffusivity and the thermal effusivity ( $e = \sqrt{\rho c_p K} = K/\sqrt{D}$ ) of the sample can be obtained<sup>24</sup> as

$$D = \frac{\pi \ell^2}{m^2}, \quad (1)$$

$$e = e_p \left( \frac{2}{\exp(d)} - 1 \right), \quad (2)$$

where  $\rho$  is the density,  $\ell$  is the sample thickness, and  $e_p$  is the thermal effusivity of the pyroelectric detector. However, at temperatures below 230 K, where the coupling grease freezes, an important piezoelectric contribution is added to the pyroelectric signal, affecting the linearity of the dependence on  $\sqrt{f}$ . This contribution has been taken into account in order to obtain reliable values of  $D$  and  $e$ .<sup>25</sup>

Once thermal diffusivity and effusivity have been measured at a certain reference temperature ( $T_{ref}$ ,  $D_{ref}$ , and  $e_{ref}$ ), the temperature is changed while recording the amplitude and phase of the pyroelectric signal at a fixed frequency. The temperature dependence of  $D$  and  $e$  are given by<sup>24,26</sup>

$$D(T) = \left( \frac{1}{\sqrt{D_{ref}}} - \frac{\Delta(T)}{\ell \sqrt{\pi f}} \right)^{-2}, \quad (3)$$

$$e(T) = e_p(T) \left( \frac{1 + \frac{e_{ref}}{e_p(T_{ref})}}{\exp[\Delta''(T)]} - 1 \right), \quad (4)$$

where  $\Delta(T) = \Psi(T) - \Psi(T_{ref})$ ,  $\Delta'(T) = \ln V(T) - \ln V(T_{ref})$ , and  $\Delta''(T) = \Delta'(T) - \Delta(T)$ . Finally, the temperature dependences of specific heat and thermal conductivity are calculated from the following relations:

$$c_p(T) = \frac{e(T)}{\rho \sqrt{D(T)}}, \quad (5)$$

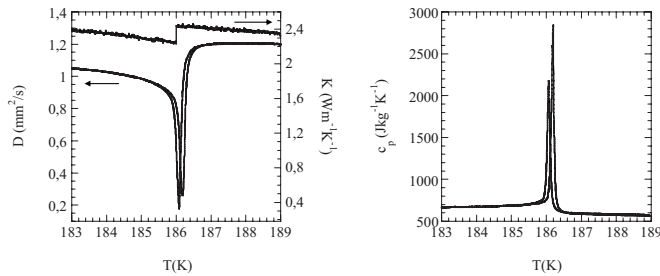


FIG. 1. Temperature dependence of  $K$ ,  $D$ , and  $c_p$  around the structural phase transition from cubic to tetragonal symmetry.

$$K(T) = e(T)\sqrt{D(T)}. \quad (6)$$

This technique is specially suited for the measurement of thermal properties around phase transitions, since small temperature gradients in the sample produce a good signal-to-noise ratio, letting thermal parameters be measured with high accuracy.

We have measured a single crystal plate of  $\text{KMnF}_3$  whose thickness is  $523 \mu\text{m}$ . Since it is transparent to the He-Ne laser, the front surface was coated with a very thin metallic layer. Its thermal properties have been measured in the temperature range from 78 to 300 K. A modulation frequency of 8.0 Hz, high enough to assure that the sample is thermally thick but low enough to guarantee a good signal-to-noise ratio, has been used. Three anomalies in the thermal properties associated with phase transitions have been observed at 186.2, 86.6, and 80.5 K. No anomaly at 91 K has been found. High-resolution measurements around each of the transition temperatures have been performed.

In Fig. 1, the temperature dependence of  $K$ ,  $D$ , and  $c_p$  around the structural phase transition from cubic to tetragonal symmetry is shown. As can be seen, a narrow and sharp dip in thermal diffusivity, together with a similarly narrow and abrupt peak in specific heat, is obtained. Both show a small thermal hysteresis of about 0.2 K. This result confirms the first order nature of this transition. On the other hand, thermal conductivity presents a small jump with no anomaly. The temperature dependence of  $D$  around the two low temperature phase transitions is shown in Fig. 2. A dip with an inverted lambda shape and no hysteresis, characteristic of a second order phase transition, has been found at the Néel temperature  $T_N=86.6$  K. On the other hand, an abrupt jump in diffusivity appears at 81 K showing a large hysteresis of about 1.5 K. This result is consistent with recent neutron diffraction measurements which demonstrate that this transition is structural first order and magnetic as well.<sup>27</sup> Our thermal measurements do not show any transition at 91 K, although it has been claimed by several authors.

#### IV. FITTING PROCEDURE AND DISCUSSION

In this section, we concentrate on the study of the critical behavior of the magnetic transition at 86.6 K. Experimental measurements of  $c_p$ ,  $D$ , and  $1/K$  in the vicinity of  $T_N$  are shown by dots in Fig. 3. As can be seen, the  $D$  values are very accurate since they are obtained directly from the phase

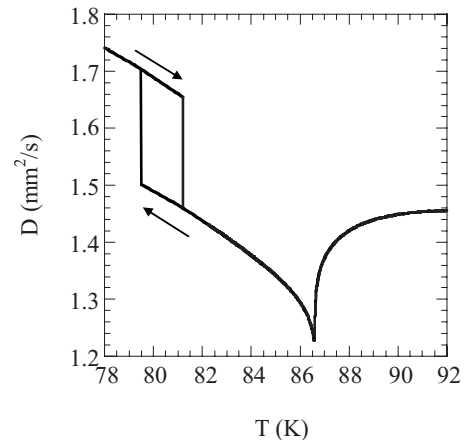


FIG. 2. Temperature dependence of  $D$  in the vicinity of the two low temperature phase transitions.

of the photopyroelectric signal [see Eq. (3)], while the  $c_p$  and  $1/K$  values are affected by a bit higher uncertainty since they are obtained by combining both amplitude and phase [see Eqs. (5) and (6)]. Note that the scale for thermal conductivity has been chosen so as to show that its singularity is much smaller than those obtained for  $D$  and  $c_p$ .

The critical behavior of the specific heat is described by a function of the form

$$c_p = B + Ct + A^\pm |t|^{-\alpha} (1 + E^\pm |t|^{0.5}), \quad (7)$$

where  $t=(T-T_N)/T_N$  is the reduced temperature, and  $\alpha$ ,  $A^\pm$ ,  $B$ ,  $C$ , and  $E^\pm$  are adjustable parameters. Superscripts  $+$  and  $-$  stand for  $T>T_N$  and  $T<T_N$ , respectively. The linear term represents the background contribution to the specific heat,

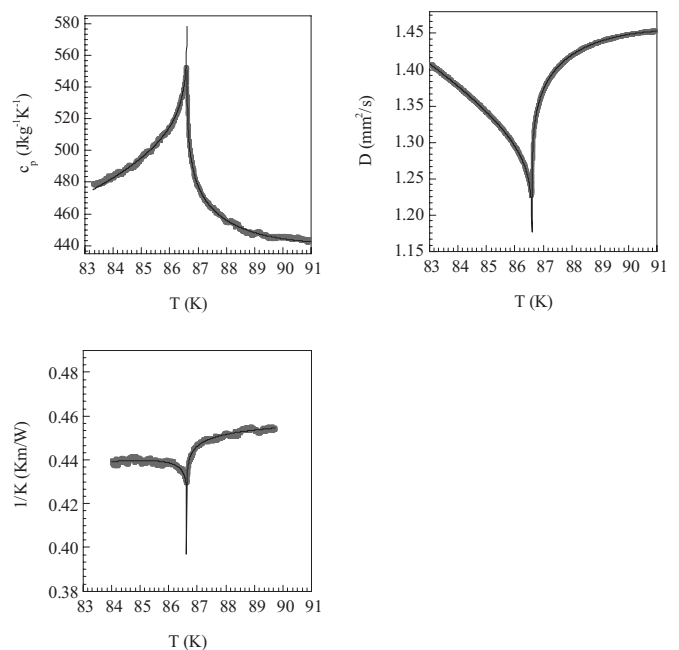


FIG. 3. Temperature dependence of  $c_p$ ,  $D$ , and  $1/K$  in the vicinity of  $T_N$ . Dots are the experimental results and the continuous lines correspond to the best fits.

while the last term is the anomalous contribution to the specific heat. The factor inside parentheses is the correction to scaling that represents a singular contribution to the leading power as known from experiments and theory.<sup>28,29</sup>

For thermal diffusivity and thermal conductivity, we assume, similarly to the specific heat, that they are given by a sum of a regular term plus a singular one, with a correction to scale term<sup>1,5</sup>

$$D = V + Wt + U^\pm |t|^{-b}(1 + F^\pm |t|^{0.5}), \quad (8)$$

$$1/K = 1/K_{nonmag} + 1/K_{mag} = L + Mt + N^\pm |t|^{-g}(1 + H^\pm |t|^{0.5}). \quad (9)$$

Subscript *nonmag* refers to phonon-phonon scattering, umklapp, scattering with impurities, etc., while *mag* refers to the spin-phonon scattering mechanisms. The magnetic resistive term originates from the spin-lattice interaction and close to  $T_N$  from an additional term that accounts for phonon scattering by critical fluctuations of the order parameter. The reason for fitting the  $1/K$  data instead of the  $K$  ones relies on the fact that all the thermal resistances associated with the various heat conduction mechanisms in the sample are in series. In this way, the singular term in Eq. (9) can be related to the magnetic contribution to the heat conduction processes.

The data were simultaneously fitted for  $T > T_N$  and  $T < T_N$  with a nonlinear least squares routine. First of all, we selected a fitting range close to the peak (dip) while avoiding the rounding and kept the fixed value of  $T_N$ . We obtained a first fitting without the correction to scaling term and obtained a set of adjusted parameters. Afterward, we tried to increase the number of points included in the fitting, first fixing  $t_{min}$  and increasing  $t_{max}$ , and then fixing  $t_{max}$  and decreasing  $t_{min}$ . The next step was introducing the correction to scaling term trying to improve the fitting. As a last check, we let  $T_N$  be a free parameter in order to confirm the fitting. In the whole process, we focused our attention on the root mean square deviations as well as on the deviation plots, which are the plots of the difference between the fitted values and the measured ones as a function of the reduced temperature. The continuous lines in Fig. 3 represent the fittings of the experimental data to Eqs. (7)–(9). In Fig. 4, the deviation plots show the range of the reduced temperatures used in the fittings as well as their quality. The values of the fitting parameters are given in Table I.

### A. Specific heat

It is seen that the values of the critical exponent and the amplitude ratio of the specific heat are in excellent agreement with the predictions of the 3D Heisenberg model for isotropic magnets ( $\alpha = -0.11$  and  $A^+/A^- = 1.58$ ).<sup>30,31</sup> Anyway, the presence of a small anisotropy can produce a crossover from the 3D Heisenberg universality class for isotropic magnets to the 3D Ising model for uniaxial anisotropic magnets as the reduced temperature approaches zero. Following the renormalization group theory,<sup>32</sup> a crossover temperature  $t_x$ , related to the degree of anisotropy of the material, can be defined as  $|t_x| = |H_A/H_E|^{0.8}$ . Accordingly, for  $|t| > |t_x|$ , the system is expected to exhibit a 3D Heisenberg universality class, while for  $|t| < |t_x|$ , the system is expected to behave

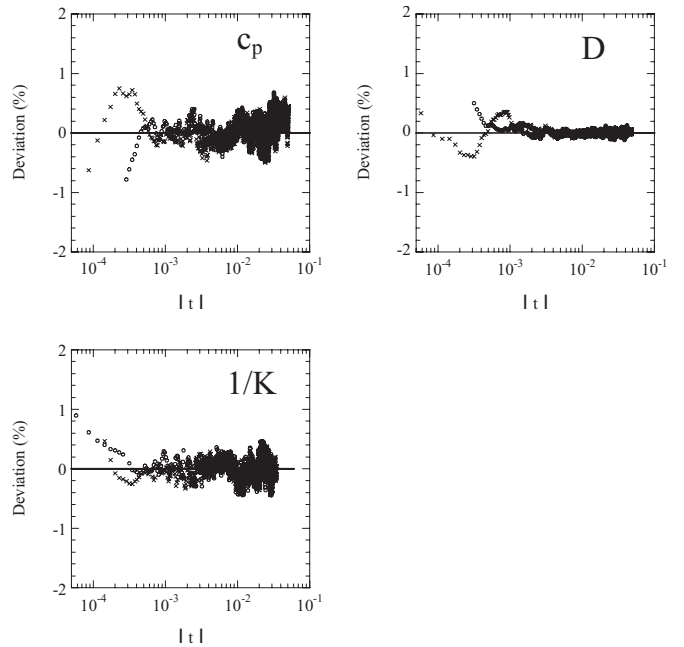


FIG. 4. Deviation plots corresponding to the fits of Fig. 3. Open circles are for  $T < T_N$  and crosses for  $T > T_N$ .

rather like a 3D Ising model. The values of  $|t_x|$  for several antiferromagnets are given in Fig. 5.<sup>12,17,18,33–37</sup> For instance,  $\text{FeF}_2$  and  $\text{CoF}_2$ , two well known uniaxial antiferromagnets, agree with the 3D Ising model in the whole critical region. On the other hand,  $\text{RbMnF}_3$ , an acknowledged isotropic antiferromagnet, agrees with the 3D Heisenberg model, since crossover to the 3D Ising model is expected only at  $|t| < 6 \times 10^{-5}$ , which has been never reached experimentally. An intermediate value appears for weakly anisotropic  $\text{Cr}_2\text{O}_3$ , for which evidence of crossover has been found as the range of the reduced temperature used in the fittings goes below  $10^{-3}$ .<sup>1,38</sup> As can be seen in Fig. 5, two different values for  $|t_x|$  are available in the literature for  $\text{KMnF}_3$ . According to the highest one, a crossover to the 3D Ising behavior should be expected for  $|t| < 1.3 \times 10^{-2}$ , and the experimental results by Akutsu and Ikeda<sup>12</sup> pointed to this crossover. However, our results support, in a wide temperature range ( $7 \times 10^{-5} - 3 \times 10^{-2}$ ), the Heisenberg model behavior and we therefore conclude that only the lowest  $t_x$  value, corresponding to  $H_A/H_E = 5.9 \times 10^{-6}$ ,<sup>18</sup> is appropriate for  $\text{KMnF}_3$ , which means an extremely weak anisotropy.

### B. Thermal diffusivity

The critical exponent and the amplitude ratio of the thermal diffusivity are very similar to those found for specific heat, a result that was already found for  $\text{RbMnF}_3$ .<sup>5</sup> Both agree with the recent predictions by Pawlak<sup>10</sup> about the critical thermal diffusivity of isotropic magnets, following the phenomenological hydrodynamical approach to critical dynamics:  $b = \alpha$  and  $U^+/U^- = A^+/A^-$ . It is worth noting that the same prediction is also found if the thermal conductivity shows no singularity at  $T_N$  or if it is very small. In such a case, using Eq. (7) for the critical behavior of  $c_p$ , the thermal diffusivity can be written as



TABLE I. Values of the adjustable fitting parameters for specific heat, thermal diffusivity, and the inverse of thermal conductivity obtained with Eqs. (7)–(9), respectively. In boldface are the universal parameters.

	$\alpha$	$A^+/A^-$	$T_N$ (K)	$B$ (J kg <sup>-1</sup> K <sup>-1</sup> )	$E$ (J kg <sup>-1</sup> K <sup>-1</sup> )	$A^-$ (J kg <sup>-1</sup> K <sup>-1</sup> )	$D^-$	$D^+$	$R$
$c_p$ (J kg <sup>-1</sup> K <sup>-1</sup> )	<b>-0.111</b> <b>±0.002</b>	<b>1.41</b> <b>±0.05</b>	86.61 ±0.01	650 ±3	4.54 ±0.07	-140 ±3	0.003 ±0.001	0.004 ±0.002	0.9985
	$b$	$U^+/U^-$	$T_N$ (K)	$V$ (mm <sup>2</sup> /s)	$W$ (mm <sup>2</sup> /s)	$U^-$ (mm <sup>2</sup> /s)	$F^-$	$F^+$	$R$
$D$ (mm <sup>2</sup> /s)	<b>-0.123</b> <b>±0.006</b>	<b>1.51</b> <b>±0.09</b>	86.60 ±0.01	1.09 ±0.01	-0.019 ±0.001	0.201 ±0.008	0.032 ±0.004	0.113 ±0.007	0.9998
	$g$	$N^+/N^-$	$T_N$ (K)	$L$ (km/W)	$M$ (km/W)	$N^-$ (km/W)	$H^-$	$H^+$	$R$
$1/K$ (Km/W)	<b>-0.10</b> <b>±0.03</b>	<b>1.15</b> <b>±0.35</b>	86.62 ±0.01	0.39 ±0.02	0.0006 ±0.0002	0.056 ±0.009	-0.10 ±0.02	-0.07 ±0.03	0.9803

$$D = \frac{K}{\rho c_p} = \frac{K}{\rho B} \left( 1 + \frac{C}{B} t + \frac{A^\pm}{B} |t|^{-\alpha} \right)^{-1}, \quad (10)$$

where we have neglected the correction to scale factor in Eq. (7), which is introduced to increase the fitting temperature range. Two universality classes will be considered.

*a. 3D Heisenberg universality* ( $A^\pm < 0$ ,  $A^+/A^- = 1.58$ , and  $\alpha = -0.11$ ). In this case as the reduced temperature approaches 0,  $|t|^{-\alpha} \ll 1$  and therefore Eq. (10) can be expanded as

$$D = \frac{K}{\rho B} \left( 1 - \frac{C}{B} t - \frac{A^\pm}{B} |t|^{-\alpha} \right) = V + Wt + U^\pm |t|^{-b}. \quad (11)$$

According to this last expression, the following relations for the universal parameters are found:  $b = \alpha = -0.11$ ,  $U^\pm = -KA^\pm/\rho B^2 > 0$ , and  $U^+/U^- = A^+/A^- = 1.58$ . Similarly, for the nonuniversal parameters, the following are found:  $V = K/\rho B$  and  $W = -KC/\rho B^2$ . Using the results of Table I we obtain for  $\text{KMnF}_3$  a good correlation between the fitted values of the thermal diffusivity parameters and those obtained from the above relations:  $b = -0.123 \approx \alpha = -0.111$ ,  $U^- = 0.200 \approx -KA^-/\rho B^2 = 0.215$ ,  $U^+/U^- = 1.51 \approx A^+/A^- = 1.41$ ,  $V = 1.09 \approx K/\rho B = 1.00$ , and  $W = -0.019 \approx -KC/\rho B^2 = -0.007$ . Only for  $W$  the discrepancy is significant, but it is due to its low value. A good correlation is also found for  $\text{RbMnF}_3$  using the fitting parameters of Table I in Ref. 5:  $b = -0.11 = \alpha = -0.11$ ,

$U^- = 0.011 \approx -KA^-/\rho B^2 = 0.014$ ,  $U^+/U^- = 1.27 = A^+/A^- = 1.27$ ,  $V = 0.067 \approx K/\rho B = 0.168$ , and  $W = -0.003 \approx -KC/\rho B^2 = -0.005$ .

*b. 3D Ising universality* ( $A^\pm > 0$ ,  $A^+/A^- = 0.50$ , and  $\alpha = +0.11$ ). Now, as the reduced temperature approaches 0,  $|t|^{-\alpha} \rightarrow \infty$  and therefore Eq. (10) reduces to

$$D = \frac{K}{\rho A^\pm} |t|^\alpha = V + Wt + U^\pm |t|^{-b}. \quad (12)$$

Accordingly, the following relations for the universal parameters are found:  $b = -\alpha = -0.11$ ,  $U^\pm = K/\rho A^\pm > 0$ , and  $U^+/U^- = A^-/A^+ = 2.00$ ; while for the nonuniversal parameters,  $V, W \rightarrow 0$ . Using the results for  $\text{FeF}_2$  in Ref. 3, a good correlation between the fitted values of the diffusivity parameters and those obtained from the above relations is found:  $b = -0.11 \approx -\alpha = -0.11$ ,  $U^- = 0.114 \approx K/\rho A^- = 0.121$ ,  $U^+/U^- = 1.97 \approx A^-/A^+ = 2.00$ ,  $V = 0.005 \ll U^- = 0.114$ , and  $W = 0.011 \ll U^- = 0.114$ .

These results together confirm the predictions of Pawlak and suggest that thermal diffusivity plays a similar role in the critical behavior as the specific heat.

### C. Thermal conductivity

As can be seen in Table I, the singular term of  $1/K$  has a positive amplitude ( $N^+, N^- > 0$ ) and a negative exponent ( $g < 0$ ), indicating that the thermal conductivity does not diverge at  $T_N$ . Moreover, the values of the critical exponent and the amplitude ratio ( $g = -0.10$  and  $N^+/N^- = 1.15$ ) are very similar to those found by Marinelli *et al.* for  $\text{RbMnF}_3$  ( $g = -0.08$  and  $N^+/N^- = 1.1$ ).<sup>5</sup> Both results are close to those expected for the 3D Heisenberg model for specific heat, although its meaning is not well understood.

Up to now, few works showing high-resolution thermal conductivity data in the vicinity of the magnetic transition temperature are available in the literature. In some of them, no singular behavior has been found, e.g.,  $\text{Cr}_2\text{O}_3$ ,  $\text{CoO}$ , and  $\text{EuO}$ .<sup>1,2,6</sup> However, in  $\text{Gd}$ , a clear dip was reported,<sup>4</sup> while a broad peak has been obtained for  $\text{FeF}_2$ ,  $\text{RbMnF}_3$ , and in the

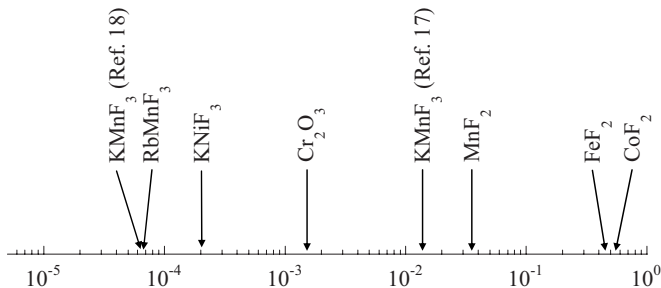


FIG. 5. Values of  $|t_x|$  for several antiferromagnets.

present work for  $\text{KMnF}_3$ .<sup>3,5</sup> These results indicate that the critical behavior of  $K$  shows a system dependency that is probably due to the different spin-phonon coupling mechanisms that are present in particular compounds. Although the reasons for the broad peak in the above mentioned magnetic fluorides are not understood in detail, we speculate that a reduction of the phonon scattering by the spin fluctuation as  $T_N$  is approached is playing an important role.

Existing theories on the critical behavior of thermal conductivity are largely incomplete. Kawasaki observed that since the heat transport is dominated by short-range processes, such as phonon scattering, no divergence should be expected for  $K$ .<sup>39</sup> Moreover, as these effects are system dependent, he suggested that the scaling laws may not hold for heat transport. The dynamic renormalization group theory<sup>9,10,40</sup> predicts that a renormalization of the bare thermal conductivity requires a contribution to the self-energy of the form  $i\omega/q^2$ , which is divergent as the wave vector  $q \rightarrow 0$  for a fixed nonzero frequency  $\omega$ . However, away from criticality, the self-energy is finite in the  $q \rightarrow 0$  limit at all orders in the perturbation theory. Thus, these perturbations which were considered so far can generate no corrections to  $K$ , and the thermal conductivity will be given exactly by its “bare” value. These results together with the few experimental data are the reasons why in modern theories of critical phenomena, the heat transport has been systematically ignored. As a consequence, even in the simple case of magnetic insulators, it is not clear which critical behavior for  $K$  should be expected.

A possible reason for the small peak in  $K$  for  $\text{FeF}_2$ ,  $\text{RbMnF}_3$ , and  $\text{KMnF}_3$  is that it could be an artifact raised by the way in which this quantity is obtained from the experimental data. From the amplitude and phase of the photopyroelectric signal, thermal diffusivity and effusivity are obtained, which, at the magnetic transition, show a dip and a peak, respectively. Then, thermal conductivity is obtained from Eq. (6). This means that close to the magnetic transition,  $K$  is the result of multiplying a peak by a dip that could produce artificial peaks or dips. However, we have measured the thermal conductivity of other magnetic materials that do not show singularity but only a small change in slope, as is the case of  $\text{CoO}$ ,  $\text{MnO}$ ,  $\text{Cr}_2\text{O}_3$ ,  $\text{Rb}_2\text{MnF}_4$ , and  $\text{KFeF}_4$ , among others.<sup>41</sup> Therefore, we conclude that the peak is real although it is much weaker than the peak in specific heat or the dip in thermal diffusivity.

Another possible explanation of the anomalous behavior of  $K$  could be the volume magnetostriction. Let us recall a simple kinetic expression for thermal conductivity,

$$K = \frac{1}{3} \sum_{q,\lambda} v_{q,\lambda} l_{q,\lambda} \frac{\partial u_{q,\lambda}}{\partial T}, \quad (13)$$

where  $v_{q,\lambda}$ ,  $l_{q,\lambda}$ , and  $u_{q,\lambda}$  denote velocity, mean free path, and energy of the phonons with wave vector  $q$ . The phonon energy density  $u_{q,\lambda} = \hbar\omega_{q,\lambda} / [V(e^{\hbar\omega_{q,\lambda}/k_B T} - 1)]$  depends on temperature explicitly through the factor  $k_B T$  and also through the volume dependence of the phonon frequencies  $\omega_{q,\lambda}(V(T))$ . The volume is temperature dependent due to the thermal expansion  $(1/V)(\partial V/\partial T) = \alpha$ , where the thermal ex-

pansion coefficient is composed of the lattice (nonsingular) and magnetic (singular) contributions:  $\alpha = \alpha_{\text{latt}} + \alpha_{\text{mag}}$ . It is the magnetostrictive coupling through which there is a singular contribution to the volume proportional to  $\langle \Phi^2 \rangle$ , where  $\Phi$  is the magnetic order parameter.<sup>10</sup> It induces anomalous contribution to  $\partial u_{q,\lambda} / \partial T$ :

$$\begin{aligned} K &= \frac{1}{3} \sum_{q,\lambda} v_{q,\lambda} l_{q,\lambda} \left[ \left( \frac{\partial u_{q,\lambda}}{\partial T} \right)_{\text{regul}} + \left( \frac{\partial u_{q,\lambda}}{\partial T} \right)_{\text{anom}} \right] \\ &= \frac{1}{3} \sum_{q,\lambda} v_{q,\lambda} l_{q,\lambda} \left[ \left( \frac{\partial u_{q,\lambda}}{\partial T} \right)_{\text{regul}} + \left( \frac{\partial u_{q,\lambda}}{\partial V} \frac{\partial V}{\partial T} \right) \right] \\ &= \frac{1}{6\pi^2} \sum_{\lambda} \int d^3 \vec{q} v_{q,\lambda} l_{q,\lambda} \frac{(\hbar\omega_{q,\lambda})^2 e^{\hbar\omega_{q,\lambda}/k_B T}}{k_B T^2 (e^{\hbar\omega_{q,\lambda}/k_B T} + 1)^2} \\ &\quad \times \left\{ 1 + \gamma_{q,\lambda} [1 - f(\hbar\omega_{q,\lambda}/k_B T)] \frac{T}{V} \frac{\partial V}{\partial T} \right\} \\ &\cong K_0 \left[ 1 + ag' \gamma^{\text{eff}} T \frac{\partial \langle \Phi^2 \rangle}{\partial T} \right], \quad (14) \end{aligned}$$

where  $\gamma_{q,\lambda} = -(V/\omega_{q,\lambda})(\partial\omega_{q,\lambda}/\partial V)$  is the Grüneisen mode parameter and  $f(\hbar\omega_{q,\lambda}/k_B T) = (k_B T/\hbar\omega_{q,\lambda}) [(e^{\hbar\omega_{q,\lambda}/k_B T} - 1)/e^{\hbar\omega_{q,\lambda}/k_B T}]$ . Only the most singular contribution to the magnetic thermal expansion has been included<sup>42</sup> (and the lattice term omitted),  $ag' \partial \langle \Phi^2 \rangle / \partial T \propto \langle \Phi^2 \rangle^2$ , which is proportional to the magnetic specific heat  $c_m$ . To sum up, the thermal conductivity has an anomalous contribution proportional to the magnetic specific heat, to the magnetostrictive coupling constant  $g'$ , and to a complicated integral from Grüneisen parameters ( $\gamma^{\text{eff}}$ ):  $K = K_0 + ag' \gamma^{\text{eff}} T c_m$ , where  $a$  is a constant. The importance of the anomalous contribution to  $K$  depends on the thermal expansion through  $g'$ . To the best of our knowledge, no thermal expansion data near the magnetic transition in  $\text{KMnF}_3$  are known. However, the dynamic elastic response of  $\text{KMn}_{1-x}\text{Ca}_x\text{F}_3$  ( $x < 0.018$ ) has been recently measured by dynamic mechanical analysis<sup>43</sup> (DMA7-Perkin Elmer) and continuous wave resonance technique around the three phase transitions.<sup>44</sup> A negative dip anomaly at  $T_N$  in the elastic constant  $C_{11}$  of about 25%, which indicates a considerable magnitude of the magnetostrictive coupling coefficient  $g'$ , has been found.

## V. CONCLUSIONS

High-resolution measurements of  $c_p$ ,  $D$ , and  $K$  around the antiferromagnetic to paramagnetic transition of  $\text{KMnF}_3$  have been performed using a photopyroelectric calorimeter. It has been found that the critical behavior of  $c_p$  agrees unambiguously with the 3D Heisenberg universality class. It means that the presence of a simultaneous phase transition from orthorhombic to tetragonal at the magnetic transition temperature does not affect the critical exponents. On the other hand, the critical exponent and the amplitude ratio of  $D$  are the same as those found for  $c_p$ , confirming the recently published theoretical predictions.<sup>10</sup> In its turn,  $K$  shows a broad peak close to the magnetic transition probably related to a reduction of the phonon scattering by the spin fluctuation in

the vicinity of  $T_N$ . Finally, we expect that these high-resolution measurements of  $K$  together with those performed in  $\text{FeF}_2$  and  $\text{RbMnF}_3$  stimulate theoretical studies on the critical behavior of this quantity in order to fill the existing void.

## ACKNOWLEDGMENTS

This work has been supported by the University of the Basque Country through research Grant No. EHU06/24 and by the Austrian FWF Project No. P19284-N20.

\*agustin.salazar@ehu.es

- <sup>1</sup>M. Marinelli, F. Mercuri, U. Zammit, R. Pizzoferrato, F. Scudieri, and D. Dadarlat, *Phys. Rev. B* **49**, 9523 (1994).
- <sup>2</sup>C. Glorieux, J. Caerels, and J. Thoen, *J. Phys. IV* **4**, 267 (1994).
- <sup>3</sup>M. Marinelli, F. Mercuri, and D. P. Belanger, *Phys. Rev. B* **51**, 8897 (1995).
- <sup>4</sup>C. Glorieux, J. Thoen, G. Bednarz, M. A. White, and D. J. W. Geldart, *Phys. Rev. B* **52**, 12770 (1995).
- <sup>5</sup>M. Marinelli, F. Mercuri, S. Foglietta, and D. P. Belanger, *Phys. Rev. B* **54**, 4087 (1996).
- <sup>6</sup>M. B. Salamon, P. R. Garnier, B. Golding, and E. Buehler, *J. Phys. Chem. Solids* **35**, 851 (1974).
- <sup>7</sup>M. Marinelli, U. Zammit, F. Mercuri, and R. Pizzoferrato, *J. Appl. Phys.* **72**, 1096 (1992).
- <sup>8</sup>M. Chirtoc, D. Dadarlat, D. Bicanic, J. S. Antoniow, and M. Egée, in *Progress in Photothermal and Photoacoustic Science and Technology*, edited by A. Mandelis and P. Hess (SPIE, Bellingham, WA, 1997), Vol. 3.
- <sup>9</sup>P. C. Hohenberg and B. I. Halperin, *Rev. Mod. Phys.* **49**, 435 (1977).
- <sup>10</sup>A. Pawlak, *Phys. Rev. B* **68**, 094416 (2003).
- <sup>11</sup>I. M. Iskornev, I. N. Flerov, N. F. Bezmaternykh, and K. S. Aleksandrov, *Zh. Eksp. Teor. Fiz.* **79**, 175 (1980).
- <sup>12</sup>N. Akutsu and H. Ikeda, *J. Phys. Soc. Jpn.* **50**, 2865 (1981).
- <sup>13</sup>A. Gibaud, S. M. Shapiro, J. Nouet, and H. You, *Phys. Rev. B* **44**, 2437 (1991).
- <sup>14</sup>G. Shirane, V. Minkiewicz, and A. Linz, *Solid State Commun.* **8**, 1941 (1970).
- <sup>15</sup>M. Hidaka, M. Ohama, A. Okasaki, H. Sakashita, and S. Yamakawa, *Solid State Commun.* **16**, 1121 (1975).
- <sup>16</sup>J. Kapusta, Ph. Daniel, and A. Ratuszna, *Phys. Rev. B* **59**, 14235 (1999).
- <sup>17</sup>S. J. Pickart, M. F. Collins, and C. G. Windsor, *J. Appl. Phys.* **37**, 1054 (1966).
- <sup>18</sup>K. Saiki, K. Horai, and H. Yoshioka, *J. Phys. Soc. Jpn.* **35**, 1016 (1973).
- <sup>19</sup>V. G. Khlyustov, I. N. Flerov, A. T. Silin, and A. N. Sal'nikov, *Sov. Phys. Solid State* **14**, 139 (1972).
- <sup>20</sup>Y. Suemune and H. Ikawa, *J. Phys. Soc. Jpn.* **19**, 1686 (1964).
- <sup>21</sup>K. Hirakawa, K. Hamazaki, H. Miike, and H. Hayashi, *J. Phys. Soc. Jpn.* **33**, 268 (1972).
- <sup>22</sup>J. Gustafson and C. Y. Walker, *Phys. Rev. B* **8**, 3309 (1973).
- <sup>23</sup>J. J. Martin, G. S. Dixon, and P. P. Velasco, *Phys. Rev. B* **14**, 2609 (1976).
- <sup>24</sup>S. Delenclos, M. Chirtoc, A. Hadj Sahraoui, C. Kolinsky, and J. M. Buisine, *Rev. Sci. Instrum.* **73**, 2773 (2002).
- <sup>25</sup>A. Salazar and A. Oleaga, *Rev. Sci. Instrum.* **76**, 034901 (2005).
- <sup>26</sup>A. Salazar, *Rev. Sci. Instrum.* **74**, 825 (2003).
- <sup>27</sup>S. Watanabe, M. Yoshimura, M. Hidaka, and H. Yoshizawa, *Appl. Phys. A: Mater. Sci. Process.* **84**, 87 (2006).
- <sup>28</sup>G. Ahlers, *Rev. Mod. Phys.* **52**, 489 (1980).
- <sup>29</sup>A. Aharony and M. E. Fisher, *Phys. Rev. B* **27**, 4394 (1983).
- <sup>30</sup>J. C. Le Guillou and J. Zinn-Justin, *Phys. Rev. B* **21**, 3976 (1980).
- <sup>31</sup>V. Privman, P. C. Hohenberg, and A. Aharony, in *Phase Transitions and Critical Phenomena*, edited by C. Domb and J. L. Lebowitz (Academic, New York, 1991), Vol. 14.
- <sup>32</sup>M. E. Fisher, *Rev. Mod. Phys.* **46**, 597 (1974).
- <sup>33</sup>M. J. Freiser, P. E. Seiden, and D. T. Teany, *Phys. Rev. Lett.* **10**, 293 (1963).
- <sup>34</sup>H. Yamaguchi, K. Katsumata, M. Hagiwara, M. Tokunaga, H. L. Liu, A. Zibold, D. B. Tanner, and Y. J. Wang, *Phys. Rev. B* **59**, 6021 (1999).
- <sup>35</sup>S. Foner, *Phys. Rev.* **130**, 183 (1963).
- <sup>36</sup>R. C. Ohlmann and M. Tinkham, *Phys. Rev.* **123**, 425 (1961).
- <sup>37</sup>F. Keffer, *Phys. Rev.* **87**, 608 (1952).
- <sup>38</sup>A. K. Murtazaev, Sh. B. Abdulgagidov, A. M. Aliev, and O. K. Musaev, *Phys. Solid State* **43**, 1067 (2001).
- <sup>39</sup>K. Kawasaki, *Prog. Theor. Phys.* **40**, 706 (1968).
- <sup>40</sup>B. I. Halperin, P. C. Hohenberg, and E. Siggia, *Phys. Rev. B* **13**, 1299 (1976).
- <sup>41</sup>A. Salazar, M. Massot, and A. Oleaga (unpublished).
- <sup>42</sup>L. R. Testardi, *Phys. Rev. B* **12**, 3849 (1975).
- <sup>43</sup>W. Schranz, A. Tröster, A. V. Kityk, P. Sondergeld, and E. K. H. Salje, *Europhys. Lett.* **62**, 512 (2003).
- <sup>44</sup>A. V. Kityk, W. Schranz, P. Sondergeld, and E. K. H. Salje (unpublished).